Dalton Transactions

ROYAL SOCIETY OF CHEMISTRY

PAPER

View Article Online
View Journal | View Issue

Check for updates

Cite this: *Dalton Trans.*, 2023, **52**, 6180

A highly conducting mixed-valence nickel bis(dithiolene) salt $[Et_4N][Ni(Me\text{-}thiazSe\text{-}dt)_2]_2$ with selone substitution†

Hadi Hachem,[a] Olivier Jeannin,[a] Hengbo Cui,[b,c] Reizo Kato,[b] Marc Fourmigué *[a] and Dominique Lorcy *[a]

Received 13th March 2023,
Accepted 14th April 2023

DOI: 10.1039/d3dt00767g

rsc.li/dalton

The prototypical $[Ni(dmit)_2]$ complex (dmit: 1,3-dithiole-2-thione-4,5-dithiolate) is modified here by combining the N–R substitution found in $[Ni(R\text{-}thiazdt)_2]$ complexes (R-thiazdt: *N*-alkyl-thiazoline-2-thione-4,5-dithiolate) and the selone substitution found in $[Ni(dmiSe)_2]$ complex (dmiSe: 1,3-dithiole-2-selone-4,5-dithiolate) to give a novel *N*-methyl substituted, radical anionic complex formulated as $[Ni(Me\text{-}thiazSe\text{-}dt)_2]^{1-}$ (Me-thiazSe-dt: *N*-methyl-thiazoline-2-selone-4,5-dithiolate). Both this anionic complex and its mixed-valence Et_4N^+ salt crystallize with a rare *cis* arrangement of the two dithiolene ligands around the Ni atom. In the 1 : 2 $[Et_4N][Ni(Me\text{-}thiazSe\text{-}dt)_2]_2$ salt, the complexes organize into dimerized chains well isolated from each other, giving the salt a strong one-dimensional character. It shows however a high RT conductivity of 4.6 S cm^{-1} and small activation energy of 33 meV, indicating a possible Mott insulator behavior, which is not suppressed under pressures up to 10 GPa.

Introduction

In the field of molecular conductors,[1] the variability offered by organic chemistry gives endless possibilities to modify at will the electroactive molecules, be they organic donor or acceptor molecules or metal complexes with chemical variations on the nature and number of ligands. In that respect, square-planar metal bis(dithiolene) complexes[2,3] provide a huge playfield as the two R^1 and R^2 substituents on the $MS_2C_2R^1R^2$ metallacycles can be engineered to control their shape and symmetry, particularly if $R^1 \neq R^2$,[4,5] or if R is chiral,[6,7] but also their HOMO/LUMO energies and HOMO–LUMO gap[8] (and associated optical properties in the NIR),[9,10] the extend of intermolecular interactions such as the S···S overlap interactions but also hydrogen[11] or halogen[12] bonding interactions. The most successful complex in these series are the $[M(dmit)_2]$ ones (Chart 1, dmit: 1,3-dithiole-2-thione-4,5-dithiolate), which provided a large number of mixed-valence conducting (and even superconducting) salts,[2,5] when associated with closed-shell (ammonium, phosphonium, sulfonium, ...) or open-shell (tetrathiafulvalenium, ferricenium, ...) cations. The dmit ligand itself can be chemically modified by atom substitution, as for example replacing the coordinating sulfur atoms by selenium ones in *diselenolene* dsit analogs,[13] or replacing the outer thione moiety by a selone one in $[M(dmiSe)_2]$ complexes (Chart 1, dmiSe: 1,3-dithiole-2-selone-4,5-dithiolate).[14]

This introduction of the selone moiety in dmiSe complexes, in place of the outer thione moiety in dmit complexes, has

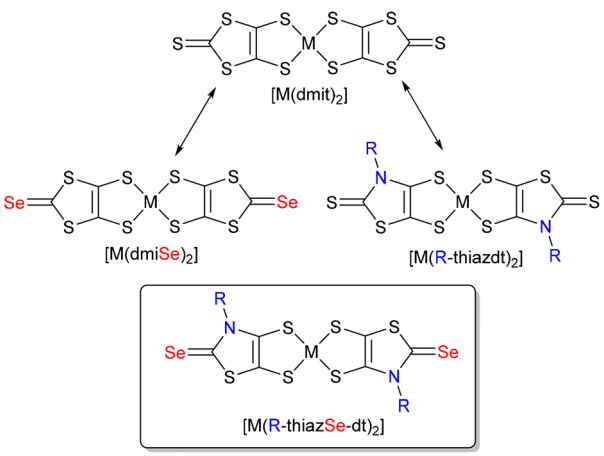

Chart 1 Chemical modifications of the dmit ligand in metal bis(dithiolene) complexes.

[a]*Université de Rennes, CNRS, ISCR (Institut des Sciences Chimiques de Rennes), F-35000 Rennes, France. E-mail: marc.fourmigue@univ-rennes1.fr, dominique.lorcy@univ-rennes1.fr*

[b]*Condensed Molecular Materials Laboratory, RIKEN, Wako-shi, Saitama 351-0198, Japan*

[c]*Department of Physics and Astronomy, Institute of Applied Physics, Seoul National University, Seoul 08826, Korea*

†Electronic supplementary information (ESI) available: Fig. S1–S3. CCDC 2246654 and 2246655. For ESI and crystallographic data in CIF or other electronic format see DOI: https://doi.org/10.1039/d3dt00767g

been investigated with the aim to increase the dimensionality of the conducting systems by favoring direct Se···Se contacts, either between face-to-face complexes within a stack or slab, or in between conducting layers, as indeed observed first in 1991 in the mixed-valence salt $[Me_4N][Ni(dmiSe)_2]_2$,[15,16] followed by other salts such as $[Me_xH_{4-x}N][Ni(dmiSe)_2]_2$ (x = 1–3) and $Cs[Pd(dmiSe)_2]_2$.[17,18]

Another modification of the dmit core is offered by the *N*-alkyl-thiazoline-2-thione-4,5-dithiolate ligand, abbreviated as R-thiazdt (Chart 1), where one of the sulfur atoms of the outer dithiole-2-thione ring is replaced by a N–R group. This substitution offers a rich palette of modifications of the dmit motif, by allowing a variety of R substituents on the nitrogen atom.[19] Also these $[M(R\text{-thiazdt})_2]^{1-}$ complexes are known to systematically oxidize at lower potentials than their dmit counterparts and in most cases the oxidation of the nickel or gold R-thiazdt monoanionic complexes doesn't afford mixed-valence salts but the neutral complexes, either the closed-shell nickel $[Ni(R\text{-thiazdt})_2]^0$ species[20] or the open-shell $[Au(R\text{-thiazdt})_2]^{\bullet}$ radicals,[19d,e,21] known as single-component conductors. Rare examples of mixed-valence derivatives have been recently reported in R-thiazoline-*diselenolene* (R-thiazds) complexes such as $[Ph_4P][Au(Me\text{-thiazds})_2]_2$,[22] or $[Et_4N][Ni(Me\text{-thiazds})_2]_2$.[23] In that respect, introduction of the selone functionality in the R-thiazdt family to give the $[M(R\text{-thiazSe-dt})_2]$ complexes (Chart 1), would combine the flexibility introduced by the R substituent on the nitrogen atom of R-thiazdt complexes with the possibility for extended intermolecular interactions observed earlier in dmiSe complexes.[15–17]

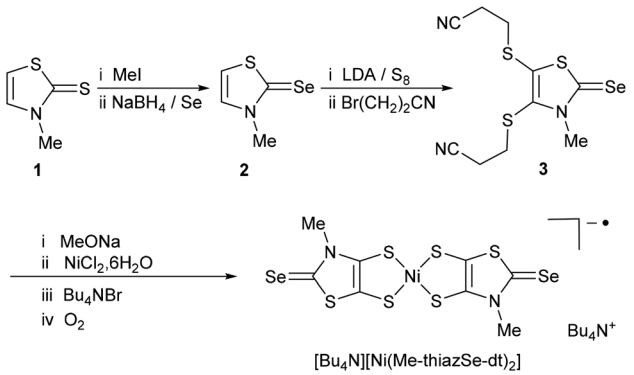

Scheme 1 Synthetic route to the anionic complex $[NBu_4][Ni(Me\text{-thiazSe-dt})_2]$.

Only two such $[M(R\text{-thiazSe-dt})_2]$ complexes have been reported earlier. The *N*-isopropyl gold complex[24] $[Au(iPr\text{-thiazSe-dt})_2]^{1-}$ was prepared for comparison with the analogous thione derivative[25] $[Au(iPr\text{-thiazdt})_2]^{1-,\bullet}$, but its electrochemical oxidation failed to provide any crystalline material, neutral or mixed-valence. The *N*-ethyl nickel complex[26] $[Ni(Et\text{-thiazSe-dt})_2]^{1-}$ was reported to oxidize to the neutral closed-shell complex $[M(R\text{-thiazSe-dt})_2]^0$, a single component semiconductor with very low conductivity ($\sigma_{RT} = 1.7 \times 10^{-5}$ S cm^{-1}), a consequence of its closed-shell character.

We describe here a novel member of this R-thiazSe-dt family, namely the *N*-methyl nickel complex $[Ni(Me\text{-thiazSe-dt})_2]^{1-}$ and demonstrate that its electrochemical oxidation leads to a highly conducting, mixed-valence 2 : 1 salt $[Et_4N][Ni(Me\text{-thiazSe-dt})_2]_2$.

Results and discussion

Syntheses and properties in solution

The preparation of the *N*-methyl anionic complex (Scheme 1) is analog to that described for the *N*-ethyl nickel complex[26] or the *N*-isopropyl gold complex.[25] It starts with the selenation of the *N*-methyl-thiazole-2-thione **1** with successively MeI and NaHSe to provide the corresponding selone **2**.[27] Metalation of **2** with LDA followed by reaction with elemental sulfur and *in situ* alkylation of the air-sensitive dithiolate with 3-bromopropionitrile provides the proligand **3** which can be easily purified and stored. Deprotection of **3** with NaOMe, reaction with $NiCl_2$, $6H_2O$ and metathesis with Bu_4NBr provides the dianionic complex which is directly oxidized in air during the recrystallization step to the monoanionic complex $[Bu_4N][Ni(Me\text{-thiazSe-dt})_2]$. As other monoanionic nickel complex, $[Ni(Me\text{-thiazSe-dt})_2]^{1-}$ exhibits a strong absorption in the NIR range, observed here at 1306 nm (ε = 25 000 M^{-1} cm^{-1}), identical to that reported for the *N*-ethyl analog (λ_{max} = 1308 nm, ε = 26 900 M^{-1} cm^{-1}).[26]

Redox properties were evaluated by cyclic voltammetry (Fig. S1 in ESI†) and results are collected in Table 1. The *N*-methyl complex exhibits similar redox potentials than its *N*-ethyl analog for the 2−/1− and 1−/0 redox processes, albeit the 1−/0 process is affected here by precipitation at the electrode, a phenomenon which was not observed with the *N*-ethyl analog. Also, the 1+/0 redox process identified in the *N*-ethyl complex at E_{pa}/E_{pc} = 0.76/0.63 V could not be observed here, a probable consequence of this decreased solubility. As already

Table 1 Redox properties of $[Ni(Me\text{-thiazSe-dt})_2]^{1-}$ and reference complexes in CH_2Cl_2 with Bu_4NPF_6 0.1 M. E in V *vs.* SCE with scan rate of 100 mV s^{-1}

Complex	$E_{pa}/E_{pc}{}^1(2-/1-)$	$E_{pa}/E_{pc}{}^2(1-/0)$	$E_{pa}/E_{pc}{}^3(0/1+)$	$\Delta E_{\frac{1}{2}}$	Ref.
$[Ni(Et\text{-thiazdt})_2]^{1-\,a}$	−0.30/−0.36	0.23/0.17	1.08/0.99	0.53	28
$[Ni(Me\text{-thiazdt})_2]^{1-\,a}$	−0.30/−0.36	0.18/−0.01	—	—	19*c*
$[Ni(Et\text{-thiazSe-dt})_2]^{1-\,b}$	−0.25/−0.31	0.27/0.21	0.76/0.63	0.52	25
$[Ni(Me\text{-thiazSe-dt})_2]^{1-\,b}$	−0.23/−0.29	0.27/0.03	—	—	This work

[a] As Ph_4P^+ salt. [b] As Bu_4N^+ salt.

observed, the introduction of the outer selone moiety (rather than the thione one in R-thiazdt complexes) leads to a higher oxidation potential for 1−/0 redox process (*cf.* Table 1). Nevertheless, electrocrystallization of the monoanionic complex was attempted in the presence of Et_4NPF_6 salt as electrolyte. In strong contrast with the oxidation of the *N*-ethyl analog which afforded the $1e^-$ oxidized *neutral* complex $[Ni(Et\text{-}thiazSe\text{-}dt)_2]^0$ (investigated as a single-component conductor),[26] the electrocrystallization of $[Ni(Me\text{-}thiazSe\text{-}dt)_2]^{1-}$ leads to a 1 : 2 mixed-valence tetraethylammonium salt formulated as $[Et_4N][Ni(Me\text{-}thiazSe\text{-}dt)_2]_2$.

Solid-state properties

The 1 : 1 salt $[Bu_4N][Ni(Me\text{-}thiazSe\text{-}dt)_2]$ crystallizes in the triclinic system, space group $P\bar{1}$, with both ions in general position in the unit cell (Fig. 2a). The ligands adopt the rare *cis* configuration around the nickel atom with a position disorder refined with a 85 : 15 occupation ratio (Fig. S2 in ESI†). The radical anions $[Ni(Me\text{-}thiazSedt)_2]^{-\bullet}$ organize into dimers, separated from each other in the structure by the bulky Bu_4N^+ cations (Fig. 1).

The plane-to-plane distance between anions within the dimers amounts to 3.56 Å, smaller than twice the sulfur van der Waals radius (3.60 Å). This lets us infer the possibility for direct antiferromagnetic interactions between the radical anions. This assumption is confirmed by the temperature dependence of the magnetic susceptibility.

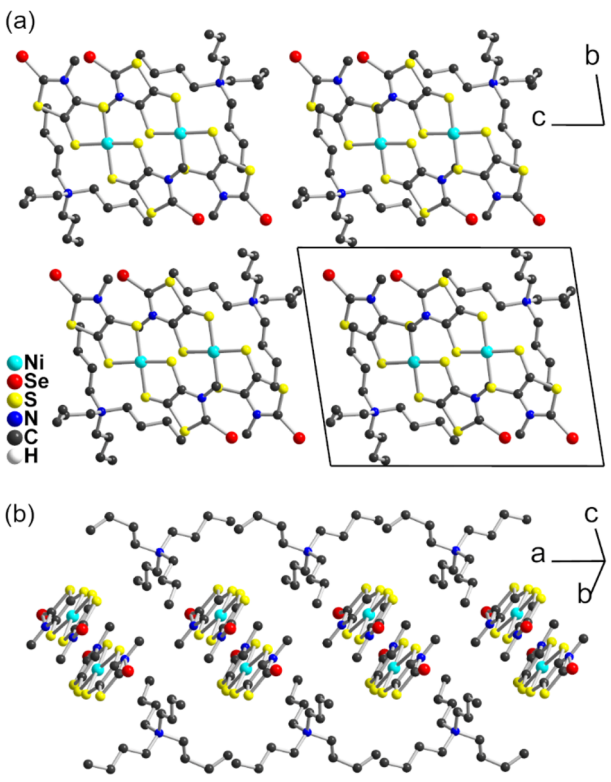

Fig. 1 (a) Projection view along the a axis of the unit cell of $[Bu_4N][Ni(Me\text{-}thiazSe\text{-}dt)_2]$; (b) organization of the dimers along the *a* axis.

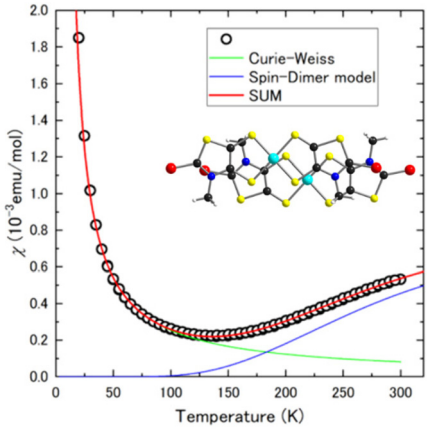

Fig. 2 Temperature dependence of the magnetic susceptibility of $[Bu_4N][Ni(Me\text{-}thiazSe\text{-}dt)_2]$. In insert, projection view perpendicular to the molecular plane of the dimer showing the overlap pattern.

As shown in Fig. 2, the susceptibility exhibits indeed an activated behavior above 100 K, together with a Curie tail at the lower temperatures. A fit considering the sum of both contributions (eqn (1)), *i.e.* the singlet–triplet contribution of the two anionic complexes and a Curie tail of magnetic defects gives a spin dimer contribution of 0.97 (close to expected $S = 1$ value, per dimer), with a J/k_B value of −668 K. The Curie contribution accounts for $x = 6.4\%$ of $S = 1/2$ magnetic defects.

$$\chi = \frac{2Ng^2\beta^2}{kT\left[3 + \exp\left(-\frac{J}{kT}\right)\right]}(1-x) + \frac{Ng^2\beta^2}{2kT}x \qquad (1)$$

The Et_4N^+ 1 : 2 mixed-valence salt obtained by electrocrystallization crystallizes in the triclinic system, space group $P\bar{1}$, with the partially oxidized complex in general position and the Et_4N^+ cation disordered on inversion center. As in the structure of the monoanionic salt (see above), the complex adopts the rare *cis* geometry, with both methyl groups pointing on the same side of the molecule. Evolutions of the intramolecular bond lengths (Table 2) from the anionic species to its partially oxidized analog are weak but doesn't follow the usual trends, *i.e.* shortening of the C–S(Ni) bonds (bonds b, b′) and lengthening of the C=C bond (bond c).

A projection view along the *a* axis (Fig. 3a) show the one-dimensional organization, with limited contacts between the stacks in the (*b*,*c*) place. Intra- and inter-stack Se···Se intermolecular distances exceeds 4.19 Å, well above the Se···Se van der Waals contact (1.90 × 2 = 3.80 Å). One single S···S interstack contact involving the sulfur atom of the thiazole rings is identified at 3.51 Å, close to the van der Waals contact distance. Within the stacks, the complexes form an alternated chain (Fig. 3b), with two different overlap patterns I and II (Fig. 3c), associated with different interplanar distances, respectively 3.54 Å (I) and 3.60 Å (II). Calculations of the $\beta_{HOMO-HOMO}$ interaction energies confirm this assumption, with $|\beta_I| = 0.23$ eV and $|\beta_{II}| = 0.19$ eV. The calculated band structure (Fig. 4) shows four bands formed out the HOMO and

Table 2 Comparison of averaged bond distances (Å) in the monoanionic $[Bu_4N][Ni(Me\text{-}thiazSe\text{-}dt)_2]$ and mixed-valence $[Et_4N][Ni(Me\text{-}thiazSe\text{-}dt)_2]_2$ salts. Both complexes are in general position, only the major component of the disordered monoanion is reported

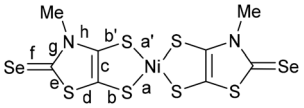

	Monoanion		Mixed-valence	
	Dist. (Å)	Aver. dist. (Å)	Dist. (Å)	Aver. dist. (Å)
a	2.169(4)	2.164	2.161(2)	2.162
	2.159(3)		2.162(2)	
a′	2.161(4)	2.161	2.169(2)	2.169
	2.161(4)		2.168(2)	
b	1.719(10)	1.670	1.682(8)	1.695
	1.622(9)		1.708(7)	
b′	1.713(10)	1.717	1.726(7)	1.718
	1.721(9)		1.710(8)	
c	1.373(16)	1.386	1.362(11)	1.365
	1.400(11)		1.368(10)	
d	1.719(10)	1.750	1.747(7)	1.741
	1.782(8)		1.735(7)	
e	1.719(9)	1.732	1.745(9)	1.748
	1.746(9)		1.751(9)	
f	1.819(8)	1.829	1.812(8)	1.806
	1.839(9)		1.800(8)	
g	1.326(10)	1.325	1.349(9)	1.350
	1.325(10)		1.351(10)	
h	1.390(11)	1.383	1.394(9)	1.392
	1.376(10)		1.390(9)	

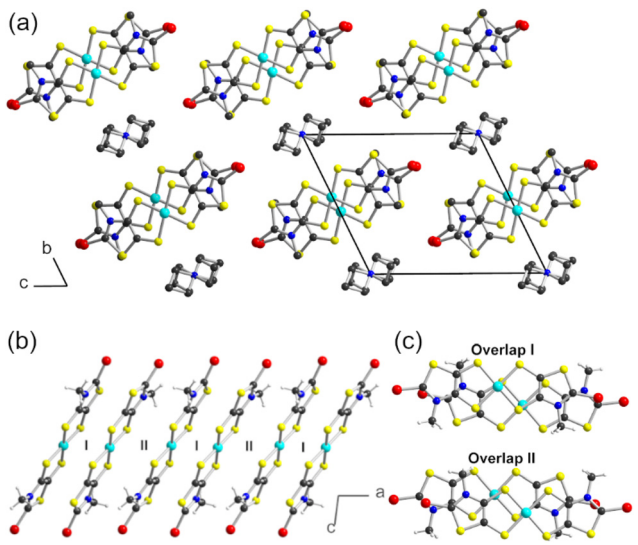

Fig. 3 Structure of $[Et_4N][Ni(Me\text{-}thiazSe\text{-}dt)_2]_2$ with (a) a projection view of the structure along the *a* axis, (b) a detail of the alternated stack of radical anions along the *a* axis with intra (I) and inter (II) dimer interactions, and (c) a detail of the I and II overlap patterns.

LUMO orbitals of both complex orientations in the solid. The third one is partially filled suggesting that this salt could be metallic, albeit its limited dispersion (0.27 eV) and strong one-dimensional character can also lead to a charge localization and associated Mott insulator behavior.

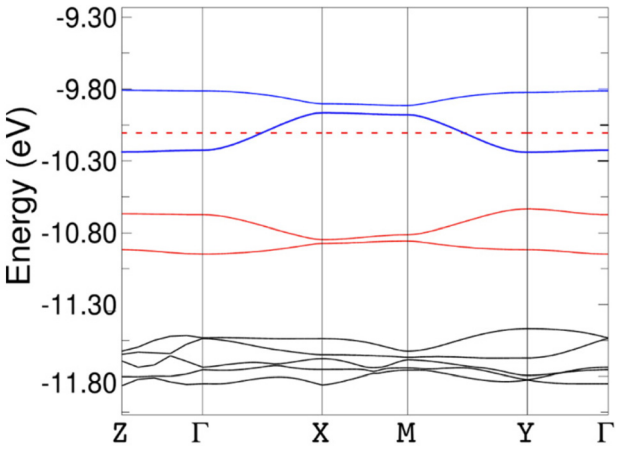

Fig. 4 Calculated band structure of $[Et_4N][Ni(Me\text{-}thiazSe\text{-}dt)_2]_2$, with the Fermi level represented by a dashed red line, assuming a metallic filling of the levels. *Γ*, *X*, *Y*, *Z*, *M*, refer respectively to *Γ* = (0, 0, 0), *X* = (1/2, 0, 0), *Y* = (0, 1/2, 0), *Z* = (0, 0, 1/2), *M* = (1/2, 1/2, 0), of the Brillouin zone of the triclinic lattice.

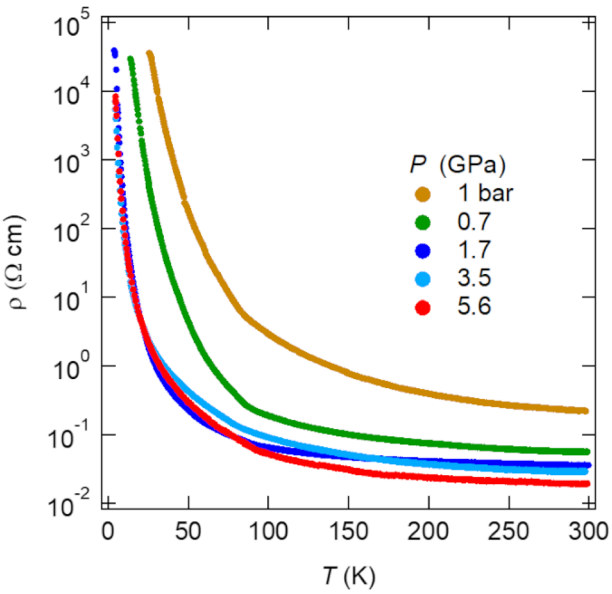

Fig. 5 Temperature and pressure dependence of the resistivity of the mixed-valence salt $[NEt_4][Ni(Me\text{-}thiazSe\text{-}dt)_2]_2$.

The temperature dependence of the resistivity is shown in Fig. 5. It exhibits an activated behavior characteristic of a semiconductor. At ambient pressure, the room temperature conductivity amounts to σ_{RT} = 4.6 S cm^{-1}, with a very small activation energy (E_{act} = 0.033 eV), in line with a Mott insulator behavior. Under such circumstances, it is often possible to close the Mott gap under pressure, as observed for example in single-component conductors derived from neutral radical gold bis(dithiolene) complexes,[19e] but also from closed-shell nickel complexes.[20,29] The evolution of the resistivity has been evaluated under pressure using a Diamond Anvil Cell (DAC) set up and is reported in Fig. 5. The RT conductivity increases

by one order of magnitude (up to 53 S cm^{-1}) at 5.6 GPa, with an activation energy divided by 2 (14 meV). At higher pressures between 5.6 and 9.8 GPa, the conductivity slightly decreases (Fig. S3 in ESI†).

The inability of this system to exhibit a metallic state under high pressures despite its mixed-valence character can be attributed here to its strong one-dimensional nature, but could be also a consequence of the disorder brought by the Et_4N^+ cation. Indeed, there are two possible routes for the occurrence of an electron localization in such systems. In the Mott-type mechanism, the electronic repulsions drive the localization of electrons, as often observed in such narrow-band systems.[30] On the other hand, the Anderson-type mechanism[31,32] is known to induce electronic localization in the presence of an extrinsic disorder, as already observed in molecular conductors.[33] Both mechanisms can be simultaneously operative in this salt.

In conclusion, we have shown here that, based on the prototypical [M(dmit)$_2$] complexes, the combination of both the N–Me substitution found in [M(Me-thiazdt)$_2$] complexes and the selone substitution found in [M(dmiSe)$_2$] complexes could afford novel nickel dithiolene complexes [Ni(Me-thiazSe-dt)$_2$] able to crystalize, upon oxidation, into mixed-valence highly conducting salts. A metallic state could not be reached in this Et_4N^+ salt, even under very high pressures (up to 10 GPa), a probable consequence of its strong 1D electronic character and possibly of the disorder introduced by the Et_4N^+ cation. We believe that the use of smaller onium salts such as Me_4N^+, Me_4P^+ or Me_3S^+ could favor stronger lateral interactions between anionic stacks and hence more two-dimensional electronic structures. Also, they might suppress the disorder problem observed here, as often, with the Et_4N^+ cation. Such systems will be investigated in a close future.

Experimental section

General

Chemicals and materials from commercial sources were used without further purification. All the reactions were performed under an argon atmosphere. Melting points were measured on a Kofler hot-stage apparatus and are uncorrected. Mass spectra were recorded by the CRMPO, Rennes. Methanol, acetonitrile and dichloromethane were dried using an Inert pure solvent column device.

Syntheses

***N*-Me-1,3-thiazoline-2-selone (2).** To a solution of *N*-Me-1,3-thiazoline-2-thione[27] **1** (2 g, 15.2 mmol) in dry acetonitrile (50 mL), iodomethane (1.9 mL, 30.4 mmol) was slowly added. The reaction was stirred at 50 °C for 12 hours under inert atmosphere. The solution was then evaporated affording a crystalline solid. The solid was added to a freshly prepared solution of NaHSe prepared from sodium borohydride (1.3 g, 34.3 mmol) and selenium powder (2.4 g, 30.4 mmol) in ethanol under inert atmosphere. After stirring for 1 hour, the solution was added to a 10% acetic acid solution (100 mL). Ethanol was evaporated and the medium was extracted with dichloromethane. The organic phase was washed with water (2 × 200 mL) and dried over $MgSO_4$. The solvent was then evaporated affording **2** as white powder. Yield: 96%; mp = 70 °C (lit.[27] 69–70 °C); R_f = 0.48 (SiO_2, CH_2Cl_2); ^{1}H NMR (300 MHz) δ: 7.19 (d, J = 4.4 Hz, 1H, CH), 6.83 (d, J = 4.4 Hz, 1H, CH), 3.80 (s, 3H, CH_3); ^{13}C NMR (75 MHz) δ: 40.6 (CH_3), 116.1 (C═C), 134.9 (C═C), 180.5 (C═Se).

4,5-Bis(2-cyanoethylthio)-*N*-methyl-1,3-thiazoline-2-selone (3). To a −10 °C cooled solution of **2** (1 g, 5.4 mmol) in dry THF (60 mL) was added a freshly prepared LDA solution in THF (8.3 mmol). After stirring for 30 min at −10 °C, sulfur (0.26 g, 8.2 mmol) was added and the solution was stirred for an additional 30 min. To the medium, LDA (11.1 mmol) was added, the reaction was then stirred at −10 °C for 3 h, followed by addition of sulfur (0.35 g, 11.1 mmol). After 30 min, 3-bromopropionitrile (4.5 mL, 54 mmol) was added dropwise and the reaction mixture was stirred overnight at RT. The solvent was evaporated *in vacuo*, and the residue was extracted with CH_2Cl_2. The organic phase was then washed with water and dried over $MgSO_4$. The solvent was evaporated and the concentrated solution was purified by flash chromatography on silica gel using CH_2Cl_2 as eluent to afford **3** as a dark brown powder which was recrystallized from ethanol to obtain yellowish crystals. Yield: 41%; mp = 124 °C; R_f = 0.23 (SiO_2, CH_2Cl_2); ^{1}H NMR (300 MHz) δ 3.92 (s, 3H, CH_3), 3.12 (m, 4H, CH_2), 2.73 (m, 4H, CH_2); ^{13}C NMR (75 MHz) δ 182.1 (C═Se), 137.1 (C═C), 130.0 (C═C), 117.0 (CN), 39.2 (NCH_3), 31.8 (SCH_2), 31.6 (SCH_2), 18.7 ($\underline{CH_2}CN$), 18.6 ($\underline{CH_2}CN$); HRMS (ESI) calcd for $C_{10}H_{11}N_3NaS_3{}^{80}Se^+$: 371.91725, found: 371.9172; Elem. anal. calcd for $C_{10}H_{11}N_3S_3Se$: C, 34.48; H, 3.18; N, 12.06. Found: C, 34.56; H, 2.99; N, 12.08.

[Bu_4N][Ni(Me-thiazSe-dt)$_2$]. Under inert atmosphere, a solution of sodium methanolate in MeOH (40 mg, 1.74 mmol in MeOH: 20 mL) was added to the proligand **3** (190 mg, 0.55 mmol). After complete dissolution, the solution was stirred at room temperature for 30 mn. Then a solution of $NiCl_2$,$6H_2O$ (66 mg, 0.27 mmol) in MeOH (5 mL) was added, followed 6 hours later by the addition of Bu_4NBr (180 mg, 0.56 mmol). After stirring for 15 h, the formed precipitate was filtered and recrystallized under air from CH_2Cl_2/MeOH 20/80 to afford the monoanionic complex as dark red crystals. Yield: 54% (120 mg); mp = 188 °C; MS (TOF MS ES) calcd for $[C_8H_6N_2NiS_6Se_2]^-$: 539.65 found: 539.65; Elem. anal. calcd for $C_{24}H_{42}N_3NiS_6Se_2$: C, 36.88; H, 5.42; N, 5.38. Found: C, 36.32; H, 5.18; N, 5.36.

Electrocrystallization

Under inert conditions in a U shaped electrocrystallization cell equipped with Pt electrodes, Et_4NPF_6 (200 mg) and the electro active monoanionic complex [Bu_4N][Ni(Me-thiazSe-dt)$_2$] (10 mg) were dissolved in CH_3CN/CH_2Cl_2 (90 : 10, 15 mL). The current intensity was adjusted to 0.5 μA between the electrodes, and the reaction was left during five days at room temp-

Table 3 Crystallographic data[a,b]

	$[Bu_4N]$ [Ni(Me-thiazSe-dt)$_2$]	$[Et_4N]$ [Ni(Me-thiazSe-dt)$_2$]$_2$
CCDC	2246654†	2246655†
Formulae	$C_{24}H_{42}N_3NiS_6Se_2$	$C_{12}H_{16}N_{2.50}NiS_6Se_2$
FW (g mol^{-1})	781.59	604.26
System	Triclinic	Triclinic
Space group	$P\bar{1}$	$P\bar{1}$
a (Å)	8.5113(2)	8.2371(11)
b (Å)	13.2483(4)	11.5377(17)
c (Å)	15.9417(4)	12.3255(16)
α (deg)	78.770(3)	65.007(5)
β (deg)	79.406(2)	87.675(5)
γ (deg)	73.437(3)	70.068(5)
V (Å^3)	1674.19(8)	990.7(2)
T (K)	293(2)	293(2)
Z	2	2
D_{calc} (g cm^{-3})	1.550	2.026
μ (mm^{-1})	3.147	5.285
Total refls	30 948	14 609
Abs corr.	Multi-scan	Multi-scan
Uniq refls (R_{int})	8134 (0.0343)	4521 (0.0858)
Uniq refls ($I > 2\sigma(I)$)	4282	2054
R_1, wR_2	0.0703, 0.1832	0.0638, 0.1186
R_1, wR_2 (all data)	0.1431, 0.2156	0.1803, 0.1486
GOF	1.02	0.951

[a] $R_1 = ||F_o| - |F_c||/|F_o|$. [b] $wR_2 = [w(F_o^2 - F_c^2)^2]/[w(F_o^2)^2]^{1/2}$.

erature. Crystals of the mixed-valence salt were collected on the anode as black crystalline needles.

X-ray crystallography

Data collections were performed on XtaLAB AFC11 Rigaku diffractometer for $[Bu_4N][Ni(Me\text{-}thiazSe\text{-}dt)_2]$ and on an APEXII Bruker-AXS diffractometer equipped with a CCD camera for $[Et_4N][Ni(Me\text{-}thiazSe\text{-}dt)_2]_2$. Structures were solved by direct methods using the *SIR97* program,[34] and then refined with full-matrix least-square methods based on F^2 (*SHELXL-97*)[35] with the aid of the *WINGX* program.[36] All non-hydrogen atoms were refined with anisotropic atomic displacement parameters. H atoms were finally included in their calculated positions. Details of the final refinements are summarized in Table 3.

Band structure calculations

The tight-binding band structure calculations were of the extended Hückel type[37] and used a modified Wolfsberg–Helmholtz formula[38] to calculate the non-diagonal $H_{\mu\nu}$ values. All valence electrons were considered in the calculations and the basis set consisted of Slater-type orbitals of double-ζ quality for Ni, S and Se atoms, and single-ζ quality for C and H atoms. The ionization potentials, contraction coefficients and exponents were taken from previous work.[39]

Conflicts of interest

There are no conflicts to declare.

Acknowledgements

This work was supported in part by Universite de Rennes (PhD grant to H. H.). The stay of H. H. to RIKEN was supported in part by RIKEN International Program Associate and by Rennes Métropole.

References

1 P. Batail, *Chem. Rev.*, 2004, **104**, 4887–4890.
2 R. Kato, *Chem. Rev.*, 2004, **104**, 5319–5346.
3 N. Robertson and L. Cronin, *Coord. Chem. Rev.*, 2002, **227**, 93–127.
4 (*a*) D. Schallenberg, N. Pardemann, A. Villinger and W. Seidel, *Dalton Trans.*, 2022, **51**, 13681–13691; (*b*) O. Jeannin, J. Delaunay, F. Barrière and M. Fourmigué, *Inorg. Chem.*, 2005, **44**, 9763–9770; (*c*) H. Benjamin, M. L. Müller, S. Afanasjevs, K. V. Kamenev and N. Robertson, *Dalton Trans.*, 2020, **49**, 13786–13796.
5 (*a*) D. Belo and M. Almeida, *Coord. Chem. Rev.*, 2010, **254**, 1479–1492; (*b*) D. Belo, H. Alves, E. B. Lopes, M. T. Duarte, V. Gama, R. T. Henriques, M. Almeida, A. Pérez-Benítez, C. Rovira and J. Veciana, *Chem. – Eur. J.*, 2001, **7**, 511–519.
6 R. Perochon, C. Poriel, O. Jeannin, L. Piekara-Sady and M. Fourmigué, *Eur. J. Inorg. Chem.*, 2009, 5413–5421.
7 F. Pop and N. Avarvari, *Coord. Chem. Rev.*, 2017, **346**, 20–31.
8 E. Canadell, *Coord. Chem. Rev.*, 1999, **185–186**, 629–651.
9 P. Deplano, L. Pilia, D. Espa, M.-L. Mercuri and A. Serpe, *Coord. Chem. Rev.*, 2010, **254**, 1434–1447.
10 F. Camerel and M. Fourmigué, *Eur. J. Inorg. Chem.*, 2020, 508–522.
11 (*a*) S. Yokomori, S. Dekura, A. Ueda, R. Kumai, Y. Murakami and H. Mori, *J. Mater. Chem. C*, 2021, **9**, 10718–10726; (*b*) H. Hachem, N. Bellec, M. Fourmigué and D. Lorcy, *Dalton Trans.*, 2020, **49**, 6056–6064; (*c*) S. Yokomori, A. Ueda, T. Higashino, R. Kumai, Y. Murakami and H. Hatsumi, *CrystEngComm*, 2019, **21**, 2940–2948.
12 (*a*) H. Hachem, O. Jeannin, M. Fourmigué, F. Barriere and D. Lorcy, *CrystEngComm*, 2020, **22**, 3579–3587; (*b*) R. Kato, *Bull. Chem. Soc. Jpn.*, 2014, **87**, 355–374.
13 (*a*) R. M. Olk, A. Roehr, J. Sieler, K. Koehler, R. Kirmse, W. Dietzsch, E. Hoyer and B. Olk, *Z. Anorg. Allg. Chem.*, 1989, **577**, 206–216; (*b*) S. Curreli, P. Deplano, M.-L. Mercuri, L. Pilia, A. Serpe, F. Bigoli, M. A. Pellinghelli, E. Coronado, C. J. Gomez-Garcia and E. Canadell, *J. Solid State Commun.*, 2002, **168**, 653–660.
14 (*a*) H. Kobayashi, R. Kato and A. Kobayashi, *Synth. Met.*, 1991, **42**, 2495–2498; (*b*) B. Olk, R. M. Olk, J. Sieler and E. Hoyer, *Synth. Met.*, 1991, **42**, 2585–2588.
15 J. P. Cornelissen, D. Reefman, J. G. Haasnoot, A. L. Spek and J. Reedijk, *Rec. Trav. Chim. Pays-Bas*, 1991, **110**, 345–346.
16 J. P. Cornelissen, B. Pomarède, A. L. Spek, D. Reefman, J. G. Haasnoot and J. Reedijk, *Inorg. Chem.*, 1993, **32**, 3720–3726.

17 A. Sato, H. Kobayashi, T. Naito, F. Sakai and A. Kobayashi, *Inorg. Chem.*, 1997, **36**, 5262–5269.
18 R. Kato, Y.-L. Liu, H. Sawa, S. Aonuma, A. Ichikawa, H. Takahashi and N. Mori, *Solid State Commun.*, 1995, **94**, 973–977.
19 (*a*) S. Eid, M. Guerro and D. Lorcy, *Tetrahedron Lett.*, 2006, **47**, 8333–8336; (*b*) M. C. Aragoni, M. Arca, F. A. Devillanova, F. Isaia, V. Lippolis, A. Mancini, L. Pala, A. M. Z. Slawin and J. D. Woollins, *Inorg. Chem.*, 2005, **44**, 9610–9612; (*c*) S. Eid, M. Fourmigué, T. Roisnel and D. Lorcy, *Inorg. Chem.*, 2007, **46**, 10647–10654; (*d*) N. Tenn, N. Bellec, O. Jeannin, L. Piekara-Sady, P. Auban-Senzier, J. íñiguez, E. Canadell and D. Lorcy, *J. Am. Chem. Soc.*, 2009, **131**, 16961–16967; (*e*) G. Yzambart, N. Bellec, N. Ghassan, O. Jeannin, T. Roisnel, M. Fourmigué, P. Auban-Senzier, J. íñiguez, E. Canadell and D. Lorcy, *J. Am. Chem. Soc.*, 2012, **134**, 17138–17148.
20 H. Hachem, H.-B. Cui, T. Tsumuraya, R. Kato, O. Jeannin, M. Fourmigué and D. Lorcy, *J. Mater. Chem. C*, 2020, **8**, 11581–11592.
21 Y. Le Gal, T. Roisnel, P. Auban-Senzier, N. Bellec, J. íñiguez, E. Canadell and D. Lorcy, *J. Am. Chem. Soc.*, 2018, **140**, 6998–7004.
22 Y. Le Gal, H.-B. Cui, P. Alemany, E. Canadell, R. Kato, T. Roisnel, V. Dorcet, M. Fourmigué and D. Lorcy, *J. Mater. Chem. C*, 2021, **9**, 12291–12302.
23 H. Hachem, H.-B. Cui, R. Kato, P. Alemany, E. Canadell, O. Jeannin, M. Fourmigué and D. Lorcy, *Inorg. Chem.*, 2023, **62**, 4197–4209.
24 A. Filatre-Furcate, F. Barrière, T. Roisnel, O. Jeannin and D. Lorcy, *Inorg. Chim. Acta*, 2018, **469**, 255–263.
25 A. Filatre-Furcate, N. Bellec, O. Jeannin, P. Auban-Senzier, M. Fourmigué, J. íñiguez, E. Canadell, B. Brière, V. Ta Phuoc and D. Lorcy, *Inorg. Chem.*, 2016, **55**, 6036–6046.
26 H. Hachem, H.-B. Cui, R. Kato, O. Jeannin, F. Barrière, M. Fourmigué and D. Lorcy, *Inorg. Chem.*, 2021, **60**, 7876–7886.
27 N. Bellec, D. Lorcy, K. Boubekeur, R. Carlier, A. Tallec, S. Los, W. Pukacki, M. Trybula, L. Piekara-Sady and A. Robert, *Chem. Mater.*, 1999, **11**, 3147–3153.
28 A. Filatre-Furcate, N. Bellec, O. Jeannin, P. Auban-Senzier, M. Fourmigué, A. Vacher and D. Lorcy, *Inorg. Chem.*, 2014, **53**, 8681–8690.
29 H. Cui, T. Tsumuraya, T. Miyazaki, Y. Okano and R. Kato, *Eur. J. Inorg. Chem.*, 2014, 3837–3840.
30 N. F. Mott, *Metal-Insulator Transitions*, Barnes and Noble, New York, 1977.
31 P. W. Anderson, *Phys. Rev.*, 1958, **109**, 1492–1505.
32 W. Hayes and A. M. Stoneham, *Defects and Defect Processes in Non -metallic Solids*, Wiley, New York, 1985, ch. 8.
33 (*a*) K. Riedl, E. Gati and R. Valentí, *Crystals*, 2022, **12**, 1689; (*b*) M. Čulo, E. Tafra, B. Mihaljević, M. Basletić, M. Kuveždić, T. Ivek, A. Hamzić, S. Tomić, T. Hiramatsu, Y. Yoshida, G. Saito, J. A. Schlueter, M. Dressel and B. Korin-Hamzić, *Phys. Rev. B*, 2019, **99**, 045114.
34 A. Altomare, M. C. Burla, M. Camalli, G. Cascarano, C. Giacovazzo, A. Guagliardi, A. G. G. Moliterni, G. Polidori and R. Spagna, *J. Appl. Crystallogr.*, 1999, **32**, 115–119.
35 G. M. Sheldrick, *Acta Crystallogr., Sect. A: Found. Crystallogr.*, 2008, **64**, 112–122.
36 L. J. Farrugia, *J. Appl. Crystallogr.*, 2012, **45**, 849–854.
37 M.-H. Whangbo and R. Hoffmann, *J. Am. Chem. Soc.*, 1978, **100**, 6093–6098.
38 J. H. Ammeter, H.-B. Bürgi, J. Thibeault and R. Hoffmann, *J. Am. Chem. Soc.*, 1978, **100**, 3686–3692.
39 S. Curreli, P. Deplano, M.-L. Mercuri, L. Pilia, A. Serpe, F. Bigoli, M. A. Pellinghelli, E. Coronado, C. J. Gómez-García and E. Canadell, *J. Solid. State Chem.*, 2002, **168**, 653–660.